Chemical Geology 417 (2015) 273–278

Contents lists available at ScienceDirect

Chemical Geology

journal homepage: www.elsevier.com/locate/chemgeo

Reconstruction of seasonal precipitation in Hawai'i using high-resolution carbon isotope measurements across tree rings

Brian A. Schubert [a,*], Axel Timmermann [b]

[a] University of Louisiana at Lafayette, School of Geosciences, Lafayette, LA 70504, USA
[b] University of Hawaii at Mānoa, International Pacific Research Center and Department of Oceanography, Honolulu, HI 96822, USA

ARTICLE INFO

Article history:
Received 23 June 2015
Received in revised form 4 October 2015
Accepted 6 October 2015
Available online 8 October 2015

Keywords:
Carbon isotopes
Hawaii
Māmane
Precipitation
Seasonality
Tree rings

ABSTRACT

Determination of carbon isotope ($\delta^{13}C$) values of tree-ring tissue is a well-established method to reconstruct past climate variability at annual resolution, but such records are limited in tropical latitudes due to the lack of well-defined annual growth bands. Recent work has demonstrated the potential for high-resolution, intra-ring $\delta^{13}C$ records to help define ring boundaries in tropical environments and provide additional climate information at sub-annual resolution. Here we present a high-resolution, intra-ring carbon isotope ($\delta^{13}C$) record of the Hawaiian endemic species *Sophora chrysophylla* (also known as "māmane") in order to assess the ability to extract seasonal climate information from these drought tolerant trees. Tree cores were sampled from high-elevation māmane trees growing on the west side of Mauna Kea, Big Island. Across our entire dataset (1986–2008), we identified a notable decreasing linear trend in the $\delta^{13}C$ record of 0.061‰/year that can be attributed to changes in the $\delta^{13}C$ value of atmospheric CO_2 and pCO_2 concentration associated with fossil fuel burning. Correcting for these affects yields a nearly flat $\delta^{13}C$ record with a slope of −0.0075‰/year, suggesting no long-term trends in climate across the study period. We observe a quasi-periodic change in the $\delta^{13}C$ values [$\Delta(\delta^{13}C)$] measured within each ring that averages 1.09 ± 0.50‰ (±1σ, $n = 23$) in amplitude. These variations are interpreted as the intra-annual isotopic signal in tree photosynthesis. The $\delta^{13}C$ variability correlates with the visible ring structure of the sample, suggesting the presence of annual growth rings at this tropical high elevation site.
We applied these data to a model that relates the $\Delta(\delta^{13}C)$ value to seasonal changes in precipitation in order to reconstruct annual changes in total summer (May through October) and winter (November through April) precipitation at the site. Across the 23-year record (1986–2008; $n = 579$ $\delta^{13}C$ measurements), reconstructed values for the ratio of summer to winter precipitation, total summer precipitation, and total winter precipitation correlate well with rainfall data collected from a nearby weather station ($r = 0.65$, 0.36, and 0.70, respectively). These results support application of this model to reconstruct inter-annual changes in seasonal precipitation from long-term tree-ring chronologies. They also demonstrate the potential of using māmane $\delta^{13}C$ for future long-term climate reconstructions.

1. Introduction

Stable isotope measurements of tree-ring tissue have shown great potential for reconstructing past climate conditions at annual resolution (Gagen et al., 2007; Kirdyanov et al., 2008; Knorre et al., 2010; Konter et al., 2014; Loader et al., 2010; Loader et al., 2008; Loader et al., 2013; Naulier et al., 2014; Seftigen et al., 2011). New methods for high-resolution sampling across tree rings have allowed for unprecedentedly high-resolution intra-annual stable isotope records (e.g., Dodd et al., 2008; Helle and Schleser, 2004; Schollaen et al., 2014; Schulze et al., 2004) and yielded information not apparent within annually sampled records (e.g., Barbour et al., 2002; Schubert and Jahren, 2011). High-resolution sampling has shown potential for identifying annual growth rings in tropical tree species (Anchukaitis et al., 2008; Fichtler et al., 2010; Pons and Helle, 2011; Schleser et al., 2015) and identifying seasonal events such as tropical cyclones (Li et al., 2011; Miller et al., 2006) and El Niño years (Verheyden et al., 2004). However, high-resolution proxy reconstructions of past precipitation variations from the Pacific Islands are lacking. Understanding the range of naturally induced rainfall variability in this region that is rich in endemic plant (e.g., Price, 2004) and animal (e.g., Case, 1996) species, and is particularly vulnerable to projected human-induced climate change (Benning et al., 2002; Duffy, 2011; Lal et al., 2002), is crucial. Here we present high-resolution, intra-ring $\delta^{13}C$ data across the unique nitrogen fixing and drought-resistant tree, māmane (*Sophora chrysophylla*), which provides the main habitat for endangered palila birds (*Loxioides bailleui*) (Banko et al., 2002; Banko and Farmer, 2014). The wide geographical and environmental extent of māmane, which spans from near sea level to the high-elevation tree line in Hawai'i (Little and Skolmen,

* Corresponding author.
E-mail address: schubert@louisiana.edu (B.A. Schubert).

http://dx.doi.org/10.1016/j.chemgeo.2015.10.013
0009-2541/

1989), makes it an excellent species for reconstructing past precipitation variations in the region.

A previous analysis of a global dataset of high-resolution, intra-ring $\delta^{13}C$ data produced a model for quantifying the long-term average seasonal precipitation from a mix of angiosperm and gymnosperm evergreen trees (Schubert and Jahren, 2011). This dataset included limited high-resolution, intra-ring $\delta^{13}C$ data from a māmane tree growing on the upper slopes of Mauna Kea, Hawai'i and were used simply to calibrate the model. Here we expand this dataset to 579 $\delta^{13}C$ measurements across 23 tree rings to produce the first proxy reconstruction of year-to-year changes in total 6-month summer (P_s; May, June, July, August, September, and October) and total 6-month winter (P_w; November, December, January, February, March, and April) precipitation (as defined within Schubert and Jahren, 2011). The high correlation between the actual precipitation data and our reconstructed values demonstrates potential for using māmane to reconstruct long-term records of seasonal precipitation in the Hawaiian Islands.

2. Methods

The main stems of māmane trees growing on the upper slopes of Mauna Kea on the island of Hawai'i (19.83° N, 155.60° W, elevation = 2100 m) (Fig. 1A) were cored at breast height in January 2010. Growth rings representing the years 1986 through 2008 were identified by counting the tree rings within core MKM04A, which showed particularly well-defined ring anatomy (Fig. 1B). Core MKM04A was subsampled by hand using a razor blade in order to precisely follow the ringed anatomy of the wood (Fig. 1B). The slices were cut parallel to the growth bands at a median sampling resolution of 110 μm (measured with a micrometer); a total of 579 subsamples were collected across 23 years of growth (average of ~25 subsamples per growth band). We judiciously sampled at this resolution in order to obtain ~90% of the seasonal intra-ring signal (see Figure 5 within Schubert and Jahren, 2011).

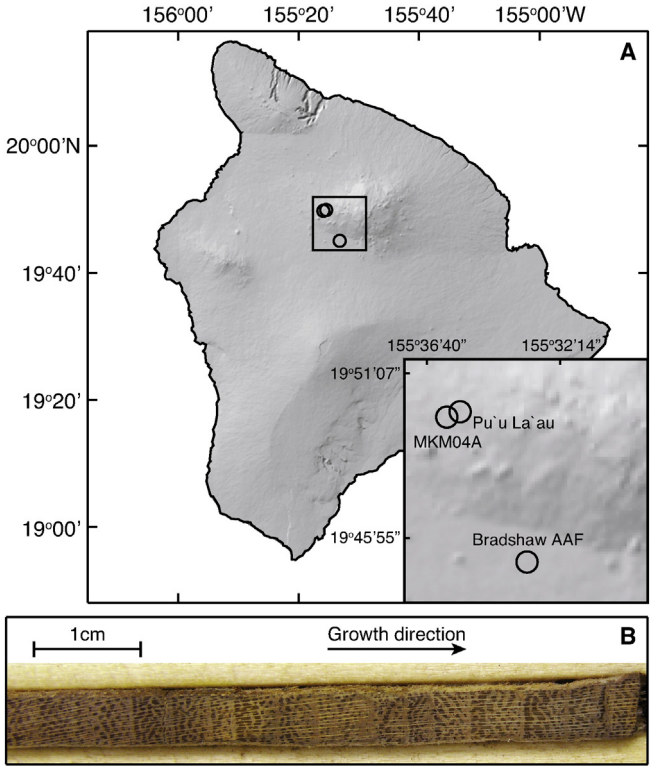

Fig. 1. (A) Digital elevation model of the island of Hawai'i showing the locations of the cored māmane tree (MKM04A) and the Pu'u La'au (precipitation) and Bradshaw Army Airfield (Bradshaw AAF; temperature) weather stations. (B) Photograph of the sampled core showing the growth bands.

Growth rates were not measured for this study; therefore, linear growth within each ring was assumed for all analyses. Bulk wood subsamples were weighed into tin capsules and $\delta^{13}C$ values were determined using a Costech ECS 4010 Elemental Analyzer (Costech Analytical, Valencia, CA, USA) in conjunction with a Thermo Delta V isotope ratio mass spectrometer (Thermo Scientific, Bremen, Germany). Samples were analyzed with two internal lab reference materials (JGLUT, $\delta^{13}C = -13.43‰$; JGLY, $\delta^{13}C = -43.51‰$) and a quality assurance sample (JRICE, $\delta^{13}C = -27.37‰$) that was analyzed as an unknown. All three materials had been previously calibrated and normalized to the VPDB scale using LSVEC and NBS-19 (Schubert and Jahren, 2012). Over the course of all analyses, the JRICE quality assurance sample averaged $-27.35 \pm 0.06‰$ (1σ, $n = 47$), which is in agreement with our calibrated value.

The site is characterized as having a temperate climate with a warm and dry summer ("Csa" Köppen–Geiger climate classification) (Peel et al., 2007). Local monthly climate data are available from nearby weather stations at Pu'u La'au (precipitation) and Bradshaw Army Airfield (AAF) (temperature) (Fig. 1A). Temperature data at Bradshaw AAF were limited to the years 1979–1990, while precipitation records for Pu'u La'au, downloaded from the Online Rainfall Atlas of Hawai'i (Giambelluca et al., 2013), extended from 1920 to 2007. Here we focus only on the precipitation data from 1986 to 2007 in order to match the period of our tree-ring record. Calculated mean annual precipitation (MAP) across this interval is 522 mm (Fig. 2A) and average monthly temperatures span a narrow range from 11.6 °C in February

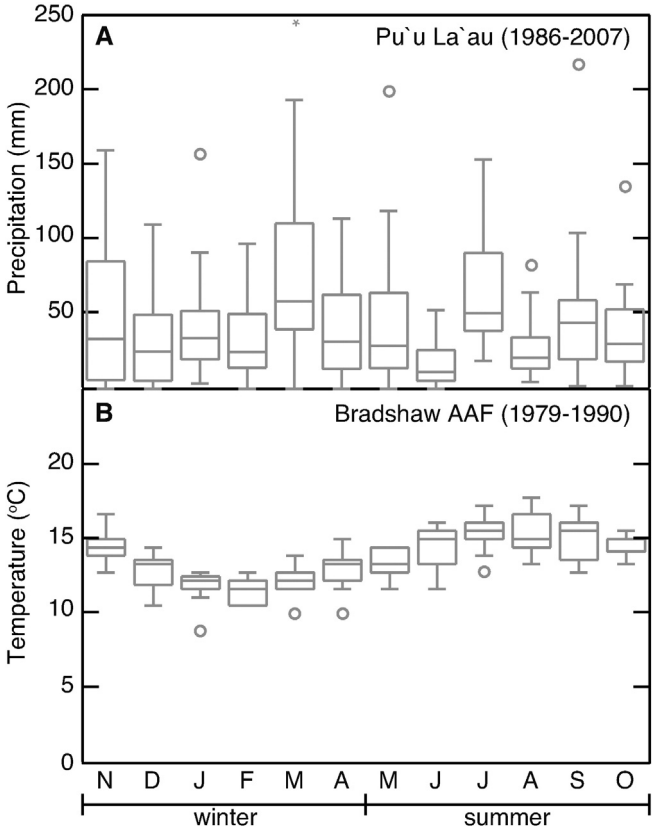

Fig. 2. Box plots showing monthly precipitation and temperature data from Pu'u La'au (1986–2007) (Giambelluca et al., 2013) and Bradshaw Army Airfield (1979–1990) (USAFETAC, 1990), respectively. (A) Monthly precipitation is highly variable from year to year and shows no clear intra-annual trends. Average winter precipitation (P_w) was 288 mm and average summer precipitation (P_s) was 234 mm. A single monthly value of 419 mm (March, 1998) is marked with an asterisk. (B) Due to the tropical latitude of the site, temperature changes throughout the year are small (only a 3.9 °C change in mean monthly temperatures throughout the year), ranging from a mean monthly temperature of 11.6 °C in February to 15.5 °C in August.

to 15.5 °C in August (Fig. 2B). Precipitation in a given month is highly variable, but on average P_w exceeds P_s (288 versus 234 mm) (Fig. 2A).

3. Results and discussion

Increment cores of māmane wood exhibit the appearance of annual growth rings (Fig. 1B). In order to test whether these rings represent an annual signal, we generate high-resolution intra-ring $\delta^{13}C$ data across a series of 23 consecutive rings; similar high-resolution $\delta^{13}C$ profiles have been used to confirm the annual nature of tree rings in other tropical tree species (e.g., Pons and Helle, 2011). The high-resolution $\delta^{13}C$ data are listed in Table S1 and shown in Fig. 3A. We observe a high frequency signal with a periodicity that corresponds to the anatomical growth bands, as well as a longer-term trend. The intra-annual $\delta^{13}C$ pattern is consistent in shape among all the rings; on average, $\delta^{13}C$ values reach a minimum near the beginning of each growth ring and a maximum in the latter half of each ring (Fig. 3B). We observe a considerable decreasing linear trend in $\delta^{13}C$ value across the study period (1986–2008) (slope = −0.61‰/decade, $r = 0.62$, $p = <0.0001$) (Fig. 3A). We adjust these raw $\delta^{13}C$ values ("$\delta^{13}C_{raw}$") to pre-industrial values ("$\delta^{13}C_{corr}$") to account for changes in the $\delta^{13}C$ value of atmospheric CO_2 ($\delta^{13}C_{CO2}$) and for changes in pCO_2 concentration using the following equation (modified from Schubert and Jahren, 2015):

$$\delta^{13}C_{corr} = \delta^{13}C_{raw} + \left[(A)(B)\left(pCO_{2(t)} + C\right)\right] / \left[A + (B)\left(pCO_{2(t)} + C\right)\right] - \left[(A)(B)\left(pCO_{2(t=0)} + C\right)\right] / \left[A + (B)\left(pCO_{2(t=0)} + C\right)\right] + \left[\delta^{13}C_{CO2(t=0)} - \delta^{13}C_{CO2(t)}\right] \quad (1)$$

where A = 28.26, B = 0.22, and C = 23.9 (after Schubert and Jahren, 2015); $\delta^{13}C_{CO2(t)}$ and $pCO_{2(t)}$ values were determined from Ferrio et al. (2005) and Keeling et al. (2001), respectively; and setting $\delta^{13}C_{CO2(t\,=\,0)} = -6.5‰$ and $pCO_{2(t\,=\,0)} = 286.7$ ppm (i.e., data for the year 1850) (see Table S1 for all input and output values). Correction for changes in $\delta^{13}C_{CO2}$ value has long been a standard procedure when interpreting $\delta^{13}C$ records (see review by McCarroll and Loader, 2004) and many studies now also adjust their $\delta^{13}C$ records for changes in pCO_2 concentration (Bégin et al., 2015; Gagen et al., 2007; Kern et al., 2013; Kirdyanov et al., 2008; Konter et al., 2014; McCarroll et al., 2009; Schollaen et al., 2013; Seftigen et al., 2011; Szymczak et al., 2012; Tei et al., 2013; Tei et al., 2014; Treydte et al., 2009; Wang et al., 2011). However, the correction for pCO_2 change is less standardized than that for $\delta^{13}C_{CO2}$. Schubert and Jahren (2012) reconciled the wide range of correction factors cited and showed that the correction for changes in pCO_2 is non-linear and dependent on the pCO_2 level in which the plant is growing. Eq. (1) uses this non-linear correction that more accurately represents the saturating effect of increasing pCO_2 on $\delta^{13}C$ than earlier linear corrections. This non-linear equation has successfully been applied to fossil leaves and organic matter (Schubert and Jahren, 2013; Schubert and Jahren, 2015), but this is the first application of this relationship to tree-rings specifically. We note that the $\delta^{13}C_{CO2}$ and pCO_2 corrected record ($\delta^{13}C_{corr}$) showed an insignificant slope of −0.015‰/decade ($r = 0.02$, $p = 0.63$), suggesting that the long-term decline observed in the raw $\delta^{13}C$ record resulted from observed changes in $\delta^{13}C_{CO2}$ and pCO_2 (and not a decrease in water stress, for example) (Fig. 3A). Consistent with this, data from Pu'u La'au show no significant increase in mean annual precipitation (i.e., a decrease in water stress, or increase in water availability; Stewart et al., 1995), across the sample period (1986–2007; $r = 0.01$, $p = 0.95$).

We interpret the intra-annual $\delta^{13}C$ pattern observed within the tree rings using the following equation modified from Eq. 9 within Schubert and Jahren (2011), which relates the intra-annual change in the $\delta^{13}C$ value [$\Delta(\delta^{13}C)$] to seasonal changes in the $\delta^{13}C_{CO2}$ value [$\Delta(\delta^{13}C_{CO2})$], post-photosynthetic physiological processes such as remobilization of stored carbon (ΔY), and the ratio of summer to winter precipitation ($R = P_s/P_w$) at the site:

$$R = e^{\wedge}\left[\left(\Delta\left(\delta^{13}C\right) - \Delta\left(\delta^{13}C_{CO2}\right) - \Delta Y\right) / -0.82\right]. \quad (2)$$

Within Eq. (2) and after Schubert and Jahren (2011), $\Delta(\delta^{13}C_{CO2}) = 0.01\,L + 0.13$ (where L is latitude) and $\Delta Y = 0.73$. $\Delta(\delta^{13}C)$ is calculated as the difference between the maximum $\delta^{13}C$ value of a given year ($\delta^{13}C_{max}$) and the preceding minimum $\delta^{13}C$ value of the annual cycle ($\delta^{13}C_{min}$). This equation assumes that the maximum and minimum $\delta^{13}C$ values of the annual cycle occurred in summer and winter, respectively, which is consistent with trees growing in tropical regions (where growth is not temperature limited) in which the climatological "wet-season" stimulates tree growth and leads to the formation of annual tree-rings (e.g., Fichtler et al., 2010). At our site, winter averages 23% more precipitation than summer (i.e., $P_s/P_w = 0.81$; Table 1), and likely drives the early season growth. Eq. (2) results from a global dataset of high-resolution $\delta^{13}C$ data on angiosperm and gymnosperm evergreen trees. Across the global dataset ($n = 15$ sites), there was very high correlation ($r = 0.98$) between the measured and predicted value for $\Delta(\delta^{13}C)$ (Schubert and Jahren, 2011). However, this result was based on long-term average climate and $\Delta(\delta^{13}C)$ data, and the interval of the climate record did not always match that of the tree-ring record; application of Eq. (2) to reconstruct year-to-year changes in seasonal precipitation has not yet been attempted.

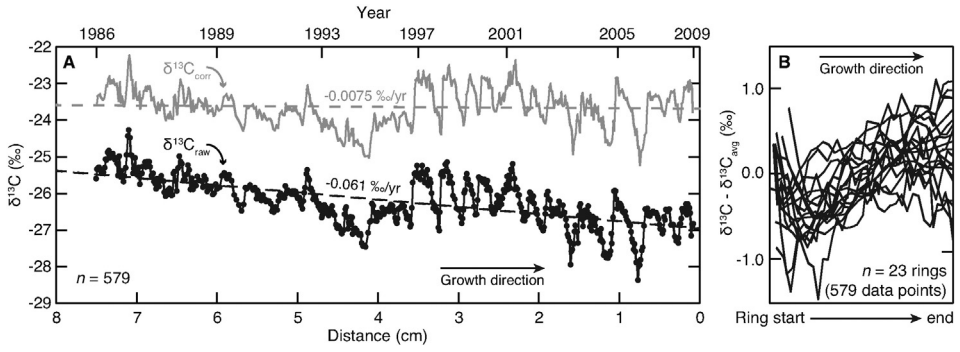

Fig. 3. High-resolution $\delta^{13}C$ measurements across māmane growth rings. Growth direction is left to right. (A) The long-term raw $\delta^{13}C$ ($\delta^{13}C_{raw}$, black) record shows a significant decrease in the $\delta^{13}C$ value from 1986 through 2008; adjusting this record for changes in $\delta^{13}C_{CO2}$ and pCO_2 attributed to fossil fuel burning using Eq. (1) yielded no long-term trend ($\delta^{13}C_{corr}$, gray). (B) Normalized intra-ring $\delta^{13}C$ data ($n = 579$) for all 23 tree rings sampled, scaled to a uniform tree-ring width, showing the general $\delta^{13}C$ pattern observed within the rings. Growth direction is from left to right; data are plotted from the start of each ring to the end of each ring. Normalized $\delta^{13}C$ values were calculated by subtracting the average $\delta^{13}C$ value for each ring ($\delta^{13}C_{avg}$) from the measured $\delta^{13}C$ value (using the "raw" $\delta^{13}C$ values). In general, the $\delta^{13}C$ value reached a maximum in the latter half of each growth ring and a minimum value within the early portion of each growth ring. Following a basic model for intra-ring $\delta^{13}C$ patterns (Schubert and Jahren, 2011), we infer that, on average, the highest $\delta^{13}C$ values occurred in summer and the lowest $\delta^{13}C$ values occurred in winter.

Table 1
Comparison between measured and reconstructed seasonal precipitation parameters.

	Pu'u La'au rainfall station				Reconstructed values		
Year	P_{total} (mm)	P_s/P_w	P_s (mm)	P_w (mm)	R[a]	P^*_s (mm)[b]	P^*_w (mm)[b]
2008	N.A.	N.A.	N.A.	N.A.	0.99	N.A.	N.A.
2007	460	0.58	168	292	1.61	283	177
2006	569	1.04	291	279	0.33	142	427
2005	841	1.14	448	393	0.39	234	607
2004	585	0.43	176	409	0.49	191	394
2003	349	0.42	104	245	0.99	173	176
2002	618	1.18	335	283	1.40	361	257
2001	426	0.60	159	267	0.70	176	251
2000	294	2.10	199	95	1.06	151	142
1999	262	1.06	135	127	0.69	107	155
1998	686	0.40	195	491	0.37	186	500
1997	811	1.01	407	404	0.47	261	550
1996	502	0.45	156	346	1.95	332	170
1995	300	1.59	184	116	0.85	138	162
1994	471	0.73	199	272	1.49	282	189
1993	344	5.18	288	56	3.64	270	74
1992	529	1.24	293	236	1.01	266	263
1991	539	0.57	197	342	1.53	326	213
1990	568	0.43	172	396	1.53	344	225
1989	753	0.83	341	412	1.77	481	272
1988	480	0.54	169	311	0.96	236	245
1987	576	0.61	219	357	0.66	229	347
1986	520	1.60	320	200	1.42	305	215
Average	*522*	*0.81*	*234*	*288*	*0.91*	*249*	*273*

N.A. = not available.
P_s = summer precipitation (May, June, July, August, September, and October).
P_w = winter precipitation (November, December, January, February, March, and April).
[a] Calculated using Eq. (2).
[b] P^*_s and P^*_w are calculated using Eqs. (4), and (5).

We test how well Eq. (2) reconstructs inter-annual changes in P_s/P_w using $\Delta(\delta^{13}C)$ values calculated for each year. Across the 23 year-long record, we find strong correlation between the actual ratio of summer to winter precipitation reported at Pu'u La'au and the reconstructed values determined using the high-resolution, intra-annual $\delta^{13}C$ data ($r = 0.65$, $p = 0.001$) (Fig. 4A). The tree-ring data show low seasonality across all years (average $P_s/P_w = 0.91$; i.e., R, Eq. (2)) with the exception of the growth ring for 1993, which yields a value of 3.64. This record is consistent with data from Pu'u La'au, which shows an average $P_s/P_w = 0.81$, and a value of 5.18 in 1993. We note that our reconstructed value for P_s/P_w (Eq. (2)) in 1993 represents a minimum value resulting from a $\Delta(\delta^{13}C)$ value of 0‰ determined from the tree-ring data for this year (no intra-annual $\delta^{13}C$ maximum was observed in this year). These results provide demonstration that Eq. (2) can be extended beyond a calculation of long-term average P_s/P_w values to reconstruct inter-annual changes in the ratio of summer to winter precipitation from intra-annual $\delta^{13}C$ records.

We can use these reconstructed values for P_s/P_w to quantify the amount of summer (P_s) and winter (P_w) precipitation provided independent data on total annual precipitation (P_{total}; here, P_{total} recorded at the Pu'u La'au station was used) and the following equation:

$$P_{total} = P_s + P_w. \quad (3)$$

By simultaneously solving Eqs. (2) and (3), values for the estimates of summer and winter precipitation, P^*_s and P^*_w, can be calculated from high-resolution, intra-ring $\delta^{13}C$ measurements:

$$P^*_w = (P_{total})/(R+1) \quad (4)$$

$$P^*_s = (R)(P_w) \quad (5)$$

where $R = P_s/P_w$ is calculated using Eq. (2). This approach has been used to reconstruct average seasonal precipitation from fossil wood (Schubert et al., 2012); it has not, however, been used to assess year-to-year changes in summer and winter precipitation. Here we use $\Delta(\delta^{13}C)$ values calculated for each year (Table 2), P_{total} data from Pu'u La'au, and Eqs. (2), (4), and (5) to quantify P_s and P_w across all 23 years of our record. We find good agreement between the actual P_s and P_w values reported at Pu'u La'au and the values calculated using our $\Delta(\delta^{13}C)$ data (Fig. 4B and 4C). We note, however, better correlation between the measured and reconstructed values for P_w ($r = 0.70$) than for P_s ($r = 0.30$) that likely results from the smaller range in summer than winter precipitation across this interval and thus the weaker correlation within the P_s data. From these data we see that the spike in P_s/P_w

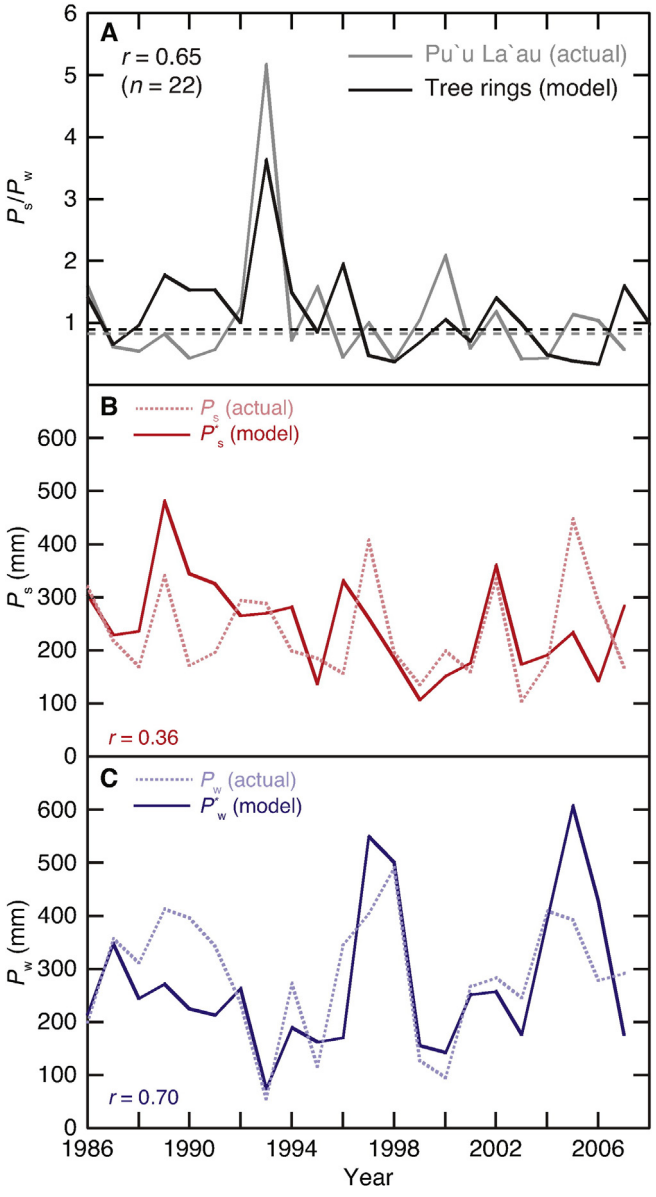

Fig. 4. Comparison of actual and reconstructed seasonal precipitation parameters. (A) Measured values for ratio of summer to winter precipitation (P_s/P_w, gray) determined using monthly precipitation data from the Pu'u La'au weather station (Giambelluca et al., 2013) compared with reconstructed values for P_s/P_w (black) calculated using $\Delta(\delta^{13}C)$ values determined for each growth ring (Table 2) and Eq. (2). The strong correlation between the measured and reconstructed values ($r = 0.65$) demonstrates the ability for high-resolution, intra-ring $\delta^{13}C$ data to be used to reconstruct year-to-year changes in P_s/P_w. Dashed lines mark average measured ($P_s/P_w = 0.81$) and reconstructed ($P_s/P_w = 0.91$) values for the study period. (B) Summer (P_s) and (C) winter (P_w) precipitation for each year were calculated using $\Delta(\delta^{13}C)$ values reported in Table 2, total annual precipitation data (P_{total}) from Pu'u La'au (Table 1), and Eqs. (4) and (5). The correlation between the actual and modeled values was better for P_w ($r = 0.70$) than for P_s ($r = 0.36$). The high correlation for P_w likely reflects the greater variability in winter than summer precipitation and the importance of winter precipitation on tree growth in this dry climate.

Table 2
Measured $\delta^{13}C$ values ($\delta^{13}C_{max}$ and $\delta^{13}C_{min}$) used to calculate $\Delta(\delta^{13}C)$.

Year	$\delta^{13}C_{max}$ (‰)	$\delta^{13}C_{min}$ (‰)	$\Delta(\delta^{13}C)$ (‰)[a]
2008	−27.35	−26.28	1.07
2007	−27.10	−26.43	0.67
2006	−28.36	−26.40	1.96
2005	−27.76	−25.92	1.84
2004	−27.94	−26.29	1.65
2003	−27.02	−25.95	1.07
2002	−26.74	−25.96	0.78
2001	−26.55	−25.20	1.35
2000	−26.57	−25.56	1.01
1999	−26.82	−25.46	1.36
1998	−27.01	−25.14	1.87
1997	−26.91	−25.24	1.67
1996	−26.82	−26.31	0.51
1995	−27.46	−26.27	1.19
1994	−27.10	−26.37	0.73
1993	−25.95	−25.95	0.00
1992	−26.41	−25.36	1.05
1991	−26.51	−25.80	0.71
1990	−26.48	−25.77	0.71
1989	−26.03	−25.44	0.59
1988	−26.07	−24.98	1.09
1987	−25.67	−24.27	1.40
1986	−25.59	−24.82	0.77

[a] $\Delta(\delta^{13}C) = \delta^{13}C_{max} - \delta^{13}C_{min}$.

calculated for the year 1993 occurs despite P_s being close to average; instead, it is the anomalously low value for P_w that drives the high summer to winter ratio. Similarly, we see that the low value for P_s/P_w in 1998 resulted from anomalously high P_w, with P_s being only slightly below average (Fig. 4B; Table 1). By combining high-resolution, intra-ring $\delta^{13}C$ data with the growing number of proxies for P_{total} [e.g., leaf-area analysis, bioclimatic analysis based upon nearest living relatives, and paleosols (Greenwood et al., 2010; Hyland et al., 2015; Wilf et al., 1998)] one could therefore gain valuable information on precipitation seasonality (summer and winter precipitation) in the fossil record. Because of the wide applicability of Eq. (2) across diverse climates, species, and geographic locations (Schubert and Jahren, 2011), analysis of ring-to-ring variability in seasonal precipitation does not require a local calibration dataset, which makes it ideal for application to sites or time periods that lack any instrumental climate data.

4. Conclusions and implications

Intra-annual changes in the $\delta^{13}C$ value of wood sectioned across radial sections of māmane trees correspond to visible changes in ring anatomy and are interpreted as annual growth bands. These intra-annual $\delta^{13}C$ records can be used to detect variations and trends in seasonal conditions, providing unique insight into the hydroclimate system of this wide-ranging, drought-resistant, tropical species. Dry conditions have been shown to contribute to declines in the critically endangered palila bird population (Banko et al., 2014), especially because these birds feed on the seeds and flowers of māmane, which are produced seasonally (Banko and Farmer, 2014) and are less abundant during drought (Banko et al., 2013).

Burning of fossil fuels since the start of the industrial revolution has resulted in a significant downward trend in tree-ring $\delta^{13}C$ values worldwide as a result of $\delta^{13}C_{CO2}$ decline and pCO_2 increase (e.g., Feng and Epstein, 1995; McCarroll et al., 2009; McCarroll and Loader, 2004; Schubert and Jahren, 2012; Treydte et al., 2009). Our raw $\delta^{13}C$ record also showed this trend, but after correcting for these affects the record was notably flat, indicating no long-term changes in water stress (for example, due to large-scale changes in precipitation) during the study period. However, our data did show variations in seasonal precipitation with accurate identification of notably wet and dry seasons (for example, the anomalously dry winter in 1993 and wet winter in 1998); summer precipitation was shown to be less variable in our dataset. The strong agreement between our reconstructed seasonal precipitation parameters and the data from a nearby rain gauge suggests that the year-to-year variability in the intra-annual $\delta^{13}C$ signal of māmane is driven by changes in stomatal conductance in response to changes in water stress. Although the negative relationship between precipitation and $\delta^{13}C$ value has been demonstrated across diverse sites using low-resolution (Fichtler et al., 2010; Gagen et al., 2006; Gebrekirstos et al., 2009; Norström et al., 2005) and high-resolution (Schubert and Jahren, 2011) sampling, this is the first inter-annual reconstruction of summer and winter precipitation using high-resolution, intra-ring $\delta^{13}C$ measurements.

Wintertime precipitation variations on Hawai'i are partly controlled by the dominant interannual-to-decadal climate modes, such as the El Niño-Southern Oscillation, the Madden–Julian Oscillation, the Pacific Decadal Oscillation, the North Pacific Gyre Oscillation, and the North Pacific Index (Chu and Chen, 2005; Diaz and Giambelluca, 2012). Although these modes have been studied extensively at a global scale, their regional manifestations for the Hawaiian Islands on timescales of centuries are less well known. Additional high-resolution $\delta^{13}C$ sampling of well-dated living or dead māmane samples holds potential for identifying these signals as they all affect seasonal precipitation patterns (Elison Timm et al., 2013). Our results demonstrate potential for māmane trees to yield high-resolution $\delta^{13}C$ data that could be used to extend records of seasonal precipitation back in time in the region at annual resolution.

Supplementary data to this article can be found online at http://dx.doi.org/10.1016/j.chemgeo.2015.10.013.

Acknowledgments

We thank W.M. Hagopian and D.C. King for laboratory assistance, Dr. A. Hope Jahren for comments on an earlier version of this manuscript and use of her stable isotope laboratory for sample preparation and analysis, Dr. Patrick Hart and Dr. Edward Cook for providing scientific guidance in sampling and coring trees in Hawai'i, and two anonymous reviewers. This work was supported by the U.S. Fish and Wildlife Service, Pacific Islands Climate Change Cooperative under award 12170-B-G103 and the Chemical Sciences, Geosciences and Biosciences Division, Office of Basic Energy Sciences, Office of Science, U.S. Department of Energy under award DE-FG02-13ER16412 (B.A.S.).

References

Anchukaitis, K.J., Evans, M.N., Wheelwright, N.T., Schrag, D.P., 2008. Stable isotope chronology and climate signal calibration in neotropical montane cloud forest trees. J. Geophys. Res. 113 (G03030). http://dx.doi.org/10.1029/2007jg000613.

Banko, P.C., Camp, R.J., Farmer, C., Brinck, K.W., Leonard, D.L., Stephens, R.M., 2013. Response of palila and other subalpine Hawaiian forest bird species to prolonged drought and habitat degradation by feral ungulates. Biol. Conserv. 157, 70–77.

Banko, P.C., Cipollini, M.L., Breton, G.W., Paulk, E., Wink, M., Izhaki, I., 2002. Seed chemistry of *Sophora chrysophylla* (mamane) in relation to diet of specialist avian seed predator *Loxioides bailleui* (palila) in Hawaii. J. Chem. Ecol. 28 (7), 1393–1410.

Banko, P.C., Farmer, C., 2014. Palila Restoration Research, 1996–2012, University of Hawai'i at Hilo. Hilo, HI.

Banko, P.C., Hess, S.C., Scowcroft, P.G., Farmer, C., Jacobi, J.D., Stephens, R.M., Camp, R.J., Leonard, D.L., Brinck, K.W., Juvik, J.O., Juvik, S.P., 2014. Evaluating the long-term management of introduced ungulates to protect the palila, an endangered bird, and its critical habitat in subalpine forest of Mauna Kea, Hawai'i. Arct. Antarct. Alp. Res. 46 (4), 871–889.

Barbour, M.M., Walcroft, A.S., Farquhar, G.D., 2002. Seasonal variation in $\delta^{13}C$ and $\delta^{18}O$ of cellulose from growth rings of *Pinus radiata*. Plant Cell Environ. 25, 1483–1499.

Bégin, C., Gingras, M., Savard, M.M., Marion, J., Nicault, A., Bégin, Y., 2015. Assessing tree-ring carbon and oxygen stable isotopes for climate reconstruction in the Canadian northeastern boreal forest. Palaeogeogr. Palaeoclimatol. Palaeoecol. 423, 91–101.

Benning, T.L., LaPointe, D., Atkinson, C.T., Vitousek, P.M., 2002. Interactions of climate change with biological invasions and land use in the Hawaiian Islands: modeling the fate of endemic birds using a geographic information system. Proc. Natl. Acad. Sci. U. S. A. 99 (22), 14246–14249.

Case, T.J., 1996. Global patterns in the establishment and distribution of exotic birds. Biol. Conserv. 78 (1–2), 69–96.

Chu, P.S., Chen, H.Q., 2005. Interannual and interdecadal rainfall variations in the Hawaiian Islands. J. Clim. 18 (22), 4796–4813.

Diaz, H.F., Giambelluca, T.W., 2012. Changes in atmospheric circulation patterns associated with high and low rainfall regimes in the Hawaiian Islands region on multiple time scales. Glob. Planet. Chang. 98-99, 97–108.
Dodd, J.P., Patterson, W.P., Holmden, C., Brasseur, J.M., 2008. Robotic micromilling of tree-rings: a new tool for obtaining subseasonal environmental isotope records. Chem. Geol. 252 (1–2), 21–30.
Duffy, D.C., 2011. No room in the ark? Climate change and biodiversity in the Pacific Islands of Oceania. Pac. Conserv. Biol. 17 (3).
Elison Timm, O., Takahashi, M., Giambelluca, T.W., Diaz, H.F., 2013. On the relation between large-scale circulation pattern and heavy rain events over the Hawaiian Islands: recent trends and future changes. J. Geophys. Res. Atmos. 118 (10), 4129–4141.
Feng, X., Epstein, S., 1995. Carbon isotopes of trees from arid environments and implications for reconstructing atmospheric CO_2 concentrations. Geochim. Cosmochim. Acta 59 (12), 2599–2608.
Ferrio, J.P., Araus, J.L., Buxó, R., Voltas, J., Bort, J., 2005. Water management practices and climate in ancient agriculture: inference from the stable isotope composition of archaeobotanical remains. Veg. Hist. Archaeobot. 14, 510–517 (http://web.udl.es/usuaris/×3845331/AIRCO2_LOESS.xls).
Fichtler, E., Helle, G., Worbes, M., 2010. Stable-carbon isotope time series from tropical tree rings indicate a precipitation signal. Tree-Ring Res. 66 (1), 35–49.
Gagen, M., McCarroll, D., Edouard, J.-L., 2006. Combining ring width, density and stable carbon isotope proxies to enhance the climate signal in tree-rings: an example from the southern French Alps. Clim. Chang. 78 (2), 363–379.
Gagen, M., McCarroll, D., Loader, N.J., Robertson, L., Jalkanen, R., Anchukaitis, K.J., 2007. Exorcising the 'segment length curse': summer temperature reconstruction since AD 1640 using non-detrended stable carbon isotope ratios from pine trees in northern Finland. The Holocene 17 (4), 435–446.
Gebrekirstos, A., Worbes, M., Teketay, D., Fetene, M., Mitlöhner, R., 2009. Stable carbon isotope ratios in tree rings of co-occurring species from semi-arid tropics in Africa: patterns and climatic signals. Glob. Planet. Chang. 66 (3–4), 253–260.
Giambelluca, T.W., Chen, Q., Frazier, A.G., Price, J.P., Chen, Y.-L., Chu, P.-S., Eischeid, J.K., Delparte, D.M., 2013. Online rainfall atlas of Hawai'i. Bull. Am. Meteorol. Soc. 94, 313–316.
Greenwood, D.R., Basinger, J.F., Smith, R.Y., 2010. How wet was the Arctic Eocene rain forest? Estimates of precipitation from Paleogene Arctic macrofloras. Geology 28 (1), 15–18.
Helle, G., Schleser, G.H., 2004. Beyond CO_2-fixation by rubisco - an interpretation of $^{13}C/^{12}C$ variations in tree rings from novel intra-seasonal studies on broad-leaf trees. Plant Cell Environ. 27 (3), 367–380.
Hyland, E.G., Sheldon, N.D., Van der Voo, R., Badgley, C., Abrajevitch, A., 2005. A New Paleoprecipitation Proxy Based on Soil Magnetic Properties: Implications for Expanding Paleoclimate Reconstructions. GSAB 127 (7/8), 975–981.
Keeling, C.D., Piper, S.C., Bacastow, R.B., Wahlen, M., Whorf, T.P., Heimann, M., Meijer, H.A., 2001. Exchanges of atmospheric CO_2 and $^{13}CO_2$ with the terrestrial biosphere and oceans from 1978 to 2000. I. Global aspectsSlO Reference Series, No. 01–06. Scripps Institution of Oceanography, San Diego.
Kern, Z., Patkó, M., Kázmér, M., Fekete, J., Kele, S., Pályi, Z., 2013. Multiple tree-ring proxies (earlywood width, latewood width and $\delta^{13}C$) from pedunculate oak (*Quercus robur* L.), Hungary. Quat. Int. 293, 257–267. http://dx.doi.org/10.1016/j.quaint.2012.05.037.
Kirdyanov, A.V., Treydte, K.S., Nikolaev, A., Helle, G., Schleser, G.H., 2008. Climate signals in tree-ring width, density and $\delta^{13}C$ from larches in eastern Siberia (Russia). Chem. Geol. 252 (1–2), 31–41.
Knorre, A.A., Siegwolf, R.T.W., Saurer, M., Sidorova, O.V., Vaganov, E.A., Kirdyanov, A.V., 2010. Twentieth century trends in tree ring stable isotopes ($\delta^{13}C$ and $\delta^{18}O$) of *Larix sibirica* under dry conditions in the forest steppe in Siberia. J. Geophys. Res. Biogeosci. 115 (G03002). http://dx.doi.org/10.1029/2009jg000930.
Konter, O., Holzkämper, S., Helle, G., Büntgen, U., Saurer, M., Esper, J., 2014. Climate Sensitivity and Parameter Coherency in Annually Resolved $\delta^{13}C$ and $\delta^{18}O$ from *Pinus uncinata* Tree-Ring Data in the Spanish Pyrenees. Chem. Geol. 377, 12–19.
Lal, M., Harasawa, H., Takahashi, K., 2002. Future climate change and its impacts over small island states. Clim. Res. 19 (3), 179–192.
Li, Z.-H., Labbé, N., Driese, S.G., Grissino-Mayer, H.D., 2011. Micro-scale analysis of tree-ring $\delta^{18}O$ and $\delta^{13}C$ on α-cellulose spline reveals high-resolution intra-annual climate variability and tropical cyclone activity. Chem. Geol. 284 (1–2), 138–147.
Little Jr., E.L., Skolmen, R.G., 1989. Common forest trees of Hawaii (native and introduced). U.S. Department of Agriculture, Forest Service, Agricultural Handbook, p. 679.
Loader, N.J., Helle, G., Los, S.O., Lehmkuhl, F., Schleser, G.H., 2010. Twentieth-century summer temperature variability in the southern Altai mountains: a carbon and oxygen isotope study of tree-rings. The Holocene 20 (7), 1149–1156.
Loader, N.J., Santillo, P.M., Woodman-Ralph, J.P., Rolfe, J.E., Hall, M.A., Gagen, M., Robertson, I., Wilson, R., Froyd, C.A., McCarroll, D., 2008. Multiple stable isotopes from oak trees in southwestern Scotland and the potential for stable isotope dendroclimatology in maritime climatic regions. Chem. Geol. 252 (1-2), 62–71.
Loader, N.J., Young, G.H.F., Grudd, H., McCarroll, D., 2013. Stable carbon isotopes from Torneträsk, northern Sweden provide a millennial length reconstruction of summer sunshine and its relationship to Arctic circulation. Quat. Sci. Rev. 62, 97–113.
McCarroll, D., Gagen, M., Loader, N.J., Robertson, I., Anchukaitis, K.J., Los, S., Young, G.H.F., Jalkanen, R., Kirchhefer, A., Waterhouse, J.S., 2009. Correction of tree ring stable isotope chronologies for changes in the carbon dioxide content of the atmosphere. Geochim. Cosmochim. Acta 73, 1539–1547.
McCarroll, D., Loader, N.J., 2004. Stable isotopes in tree rings. Quat. Sci. Rev. 23 (7–8), 771–801.
Miller, D.L., Mora, C.I., Grissino-Mayer, H.D., Mock, C.J., Uhle, M.E., Sharp, Z., 2006. Tree-ring isotope records of tropical cyclone activity. Proc. Nat. Acad. Sci. U.S.A. 103 (39), 14294–14297.
Naulier, M., Savard, M.M., Bégin, C., Marion, J., Arseneault, D., Bégin, Y., 2014. Carbon and oxygen isotopes of lakeshore black spruce trees in northeastern Canada as proxies for climatic reconstruction. Chem. Geol. 374-375, 37–43.
Norström, E., Holmgren, K., Mörth, C.M., 2005. Rainfall-driven variations in $\delta^{13}C$ composition and wood anatomy of *Breonadia salicina* trees from South Africa between AD 1375 and 1995. S. Afr. J. Sci. 101 (3–4), 162–168.
Peel, M.C., Finlayson, B.L., McMahon, T.A., 2007. Updated world map of the Köppen–Geiger climate classification. Hydrol. Earth Syst. Sci. 11 (5), 1633–1644.
Pons, T.L., Helle, G., 2011. Identification of anatomically non-distinct annual rings in tropical trees using stable isotopes. Trees Struct. Funct. 25 (1), 83–93.
Price, J.P., 2004. Floristic biogeography of the Hawaiian Islands: influences of area, environment and paleogeography. J. Biogeogr. 31 (3), 487–500.
Schleser, G.H., Anhuf, D., Helle, G., Vos, H., 2015. A remarkable relationship of the stable carbon isotopic compositions of wood and cellulose in tree-rings of the tropical species *Cariniana micrantha* (ducke) from Brazil. Chem. Geol. 401, 59–66.
Schollaen, K., Heinrich, I., Helle, G., 2014. UV-laser-based microscopic dissection of tree rings — a novel sampling tool for $\delta^{13}C$ and $\delta^{18}O$ studies. New Phytol. 201 (3), 1045–1055.
Schollaen, K., Heinrich, I., Neuwirth, B., Krusic, P.J., D'Arrigo, R.D., Karyanto, O., Helle, G., 2013. Multiple tree-ring chronologies (ring width, $\delta^{13}C$ and $\delta^{18}O$) reveal dry and rainy season signals of rainfall in Indonesia. Quat. Sci. Rev. 73, 170–181.
Schubert, B.A., Jahren, A.H., 2011. Quantifying seasonal precipitation using high-resolution carbon isotope analyses in evergreen wood. Geochim. Cosmochim. Acta 75 (22), 7291–7303. http://dx.doi.org/10.1016/j.gca.2011.08.002.
Schubert, B.A., Jahren, A.H., 2012. The effect of atmospheric CO_2 concentration on carbon isotope fractionation in C_3 land plants. Geochim. Cosmochim. Acta 96, 29–43.
Schubert, B.A., Jahren, A.H., 2013. Reconciliation of marine and terrestrial carbon isotope excursions based on changing atmospheric CO_2 levels. Nat. Commun. 4 (1653). http://dx.doi.org/10.1038/ncomms2659.
Schubert, B.A., Jahren, A.H., 2015. Global increase in plant carbon isotope fractionation following the last glacial maximum caused by increase in atmospheric pCO_2. Geology 43 (5), 435–438.
Schubert, B.A., Jahren, A.H., Eberle, J.J., Sternberg, L.S.L., Eberth, D.A., 2012. A summertime rainy season in the Arctic forests of the Eocene. Geology 40 (6), 523–526.
Schulze, B., Wirth, C., Linke, P., Brand, W.A., Kuhlmann, I., Horna, V., Schulze, E.D., 2004. Laser ablation-combustion-GC-IRMS — a new method for online analysis of intra-annual variation of $\delta^{13}C$ in tree rings. Tree Physiol. 24 (11), 1193–1201.
Seftigen, K., Linderholm, H.W., Loader, N.J., Liu, Y., Young, G.H.F., 2011. The influence of climate on $^{13}C/^{12}C$ and $^{18}O/^{16}O$ ratios in tree ring cellulose of *Pinus sylvestris* L. growing in the central Scandinavian mountains. Chem. Geol. 286 (3–4), 84–93.
Stewart, G.R., Turnbull, M.H., Schmidt, S., Erskine, P.D., 1995. ^{13}C natural abundance in plant communities along a rainfall gradient: a biological integrator of water availability. Aust. J. Plant Physiol. 22 (1), 51–55.
Szymczak, S., Joachimski, M.M., Bräuning, A., Hetzer, T., Kuhlemann, J., 2012. A 560 yr summer temperature reconstruction for the western Mediterranean basin based on stable carbon isotopes from *Pinus nigra* ssp. *laricio* (Corsica/France). Clim. Past 8 (5), 1737–1749.
Tei, S., Sugimoto, A., Yonenobu, H., Hoshino, Y., Maximov, T.C., 2013. Reconstruction of summer palmer drought severity index from $\delta^{13}C$ of larch tree rings in east Siberia. Quat. Int. 290–291, 275–281.
Tei, S., Sugimoto, A., Yonenobu, H., Ohta, T., Maximov, T.C., 2014. Growth and physiological responses of larch trees to climate changes deduced from tree-ring widths and $\delta^{13}C$ at two forest sites in eastern Siberia. Polar Sci. 8 (2), 183–195.
Treydte, K.S., Frank, D.C., Saurer, M., Helle, G., Schleser, G.H., Esper, J., 2009. Impact of climate and CO_2 on a millennium-long tree-ring carbon isotope record. Geochim. Cosmochim. Acta 73, 4635–4647.
USAFETAC, 1990. Surface Observation Climatic Summaries (SOCS) for Bradshaw AAF Hawaii, United States Air Force Environmental Technical Applications Center, USAFETAC/DS-90/225.
Verheyden, A., Helle, G., Schleser, G.H., Dehairs, F., Beeckman, H., Koedam, N., 2004. Annual cyclicity in high-resolution stable carbon and oxygen isotope ratios in the wood of the mangrove tree *Rhizophora mucronata*. Plant Cell Environ. 27 (12), 1525–1536.
Wang, W., Liu, X., Shao, X., Leavitt, S., Xu, G., An, W., Qin, D., 2011. A 200 year temperature record from tree ring $\delta^{13}C$ at the Qaidam basin of the Tibetan Plateau after identifying the optimum method to correct for changing atmospheric CO_2 and $\delta^{13}C$. J. Geophys. Res. 116, G04022.
Wilf, P., Wing, S.L., Greenwood, D.R., Greenwood, C.L., 1998. Using fossil leaves as paleoprecipitation indicators: an Eocene example. Geology 26, 203–206.